Rapid Detection and Location of Debris Flow Initiation at Illgraben, Switzerland

Fabian Walter[1,2], Arnaud Burtin[3,4], Brian McArdell[2], Niels Hovius[3], Bianca Weder[1] and Jens M. Turowski[3]

[1]Laboratory of Hyrdaulics, Hydrology and Glaciology, ETH Zurich, 8093, Switzerland
[2]Swiss Federal Institute for Forest, Snow and Landscape Research WSL, 8903, Switzerland
[3]GFZ German Research Centre for Geosciences, 14473, Germany
[4]Institut de Physique Du Globe de Paris, 75238, France

Correspondence to: Fabian Walter (walter@vaw.baug.ethz.ch)

Abstract. Heavy precipitation can suddenly mobilize tens to hundreds of thousands of cubic meters of sediments in steep Alpine torrents. The resulting debris flows (mixtures of water, sediments and boulders) move downstream with velocities of several meters per second and have a high destructive potential. Warning schemes for affected communities rely on raising awareness to the debris flow threat, precipitation monitoring and rapid detection methods. The latter, in particular, remain an ongoing challenge, because debris-flow-prone torrents have their catchments in steep and inaccessible terrain, where installing and maintaining instrumentation is difficult. Here, we propose a simple processing scheme for seismic network data. We use debris flow and noise seismograms from Illgraben, Switzerland, a torrent, which produces several debris flow events per year. Automatic in-situ detection is currently based on geophones mounted on concrete check dams and radar stage sensors hung above the channel. The proposed approach has the advantage that it uses seismometers, which can be installed at more accessible locations, and where a stable connection to portable phone networks is available for data communication. Our data processing uses time-averaged ground vibration amplitudes to estimate the location of the debris flow front. Applied to continuous data streams, inversion of the seismic amplitude decay eliminates the need for single-station-based detection and knowledge of the local seismic velocity model. This makes the approach suitable for automation, as seismic phase identification is unnecessary and the amplitude averaging significantly reduces data volume. We apply our approach to a small debris flow event on 19 July 2011, which was captured with a temporary monitoring network. The processing rapidly detects the debris flow event half an hour before its front arrives at the torrent mouth and 8 minutes before detection by the current alarm system. An analysis of continuous seismic records furthermore indicates that detectability of Illgraben debris flows of this size are unaffected by changing environmental and cultural seismic noise. We therefore propose that our method reliably detects initiation of the Illgraben debris flows and can thus form an important ingredient in the next generation of early warning schemes.

1 Introduction

Triggered by heavy precipitation events, debris flows threaten human lives and infrastructure in Alpine regions, including Switzerland (e.g. Rickenmann and Zimmermann, 1993). Their destructive potential demands warning measures for local communities. Several approaches exist, such as rainfall forecasts and real-time precipitation monitoring, which trigger an

5   alarm once a certain threshold is exceeded (e.g., Wieczorek 1987; Deganutti et al. 2000; Fan et al. 2003). However, whereas precipitation-based alarm is useful to raise the general level of alert, it is often not accurate enough to serve as a basis for rescue deployment, road closure or building evacuation. For such measures, it is necessary to communicate debris flow initiation in a torrent's upper catchment with minimal time delays. This requires reliable instrument installation and operation in difficult and often unstable terrain in torrent catchments. Implementation of warning systems against debris flows

10   therefore remains a significant technical challenge.

Seismological techniques constitute a promising approach to tackle this challenge, because Alpine mass movements typically involve processes that generate seismic waves detectable at kilometer distances (Burtin et al., 2016). Ground impact of rock falls (Deparis et al., 2008), particle hopping during bedload transport in rivers (Burtin et al., 2008; Tsai et al.,

15   2012) and snow avalanche or landslide interaction with obstacles (Surinach et al., 2000, Dammeier et al., 2011) all transmit high frequency (>1 Hz) seismic energy to the ground. Consequently, with the advent of more portable sensor and recorder technology, seismology has been becoming increasingly popular in natural hazard research. Unlike landslides, avalanches and rock falls, debris flows move at relatively slow velocities below 10 m/s (e.g. Hürlimann et al., 2003). In principle, seismic monitoring thus allows for considerable warning time provided that detection occurs rapidly upon debris flow

20   initiation.

Recent studies have documented a clear seismic footprint of debris flows. Near a torrent bed, debris flows induce ground vibration of up to 2×10^{-3} m/s (Hübl et al., 2013) over a frequency spectrum between a few and nearly 100 Hz (Burtin et al., 2013). This has allowed detection of the debris flow front up to 50 s before its arrival, which can be improved with the

25   additional sensing of sound waves traveling through air (Arratano and Marchi, 2005; Hübl et al., 2013; Schimmel and Hübl, 2015).

These developments suggest a high potential for seismology-based early warning or rapid response systems (Manconi et al., 2016). Nevertheless, a reliable implementation for debris flows has yet to be found. Proposed single-station detection

30   schemes require site-specific parameter tuning, which inhibit transfer to other debris flow torrents and may yield false alarms in the presence of additional seismic sources, such as anthropogenic noise (Schimmel and Hübl, 2015; Burtin et al., 2013; Arratano et al., 2014). As an alternative, the advantages of network seismology should be leveraged to associate detections on various stations with a single (debris flow) source. Larger seismometer networks installed throughout an entire torrent

catchment (e.g. Burtin et al., 2013) allow instrumentation at greater distances from the torrent. Although near-torrent seismometers can measure arrivals and velocities of the debris flow front (Arattano, 1999; Arattano and Marchi, 2005; Burtin et al., 2016), such installations are difficult and potentially dangerous in the upper catchments of debris flow-prone-torrents. In any case, moving instruments away from the torrent and confining the analysis to lower frequencies reduces the influence of structural site effects on ground motion (Hürlimann et al., 2003).

Here we propose a simple processing approach of seismic data from the Illgraben catchment, Switzerland. This torrent produces several debris flow events per year, which threaten human activity and in extreme cases have destroyed infrastructure in the Rhone valley. We use data from a campaign seismic network (Burtin et al., 2013) installed throughout the torrent catchment and primarily in locations were the Global System for Mobile Communication ("GSM") network can be accessed for data transfer and where enough sunlight for instrument power consumption is available. The proposed detection scheme identifies locations of dominant seismic signals in the torrent region by modeling the amplitude decay throughout the seismic network. A seismic noise analysis from a summer record in the Rhone Valley indicates that this method is robust with respect to changes in seismic background noise. The additional warning time found for the investigated debris flow may therefore be representative for other events.

2 Illgraben Debris Flows

The Illgraben drains a catchment of 10 km^2 (Fig. 1) and transports large amounts of sediment to the Rhone river, as is testified by the large, debris fan in the Rhone valley. Hosting the village of Susten, this partially inhabited debris fan has a radius of nearly 2 km. On yearly average, Illgraben delivers nearly 100,000 m^3 of sediments to the Rhone. A large portion of the sediment transfer occurs during debris flow events making the Illgraben the most active debris flow torrent in Switzerland (Rickenmann, 2001).

Debris flow granulometry and water content varies between individual events, but they are generally characterized by boulder-rich fronts carrying little matrix soil debris and an event main body made up of a finer mixture of liquefied soil debris (Pierson 1986; Badoux et al., 2009). Illgraben debris flows reach velocities of 4-8 m/s in the lower channel portions and have flow heights of up to 2-3 m (Badoux et al., 2009; WSL, unpublished data). Their volumes range from order 10^3 to 10^5 m^3, while "small " events not exceeding a few tens of 10^3 m^3 occur up to 8 times per year and are thus most frequent (Hürlimann et al., 2003). Volumes between 75,000 m^3 and 250,000 m^3 are classified as "intermediate size". Such events occur several times per century and may locally overtop the channel banks. Events classified as "large" can potentially reach populated areas outside the Illgraben channel and therefore have a particularly high damage potential. This case occurred in 1961 when the largest documented event of 500,000 m^3 destroyed a road bridge on the fan (Badoux et al., 2009). Although

no channel overtopping has occurred since at least 2000, even smaller debris flow events constitute a threat to lives of people crossing the channel during professional or recreational activities.

Illgraben debris flows are believed to initiate in the sub-catchment area in the south-west of the catchment (outlined in
5 Figure 1). Here, erosion on the steep lateral slopes (on average 40°) mobilizes sediments that are subsequently delivered to the Illgraben channel, which are then mobilized to debris flows during intense thunderstorms typically occurring from April to October. The largest debris flow events are expected when temporary creek dams produced by landslides from the steep lateral slopes suddenly fail (Badoux et al., 2009). Much of the debris flow initiation and propagation effects are not fully understood, because the debris flows interact with their surroundings by eroding the Illgraben channel bed (Berger et al.,
10 2011) and the channel banks, which in turn may recharge ongoing or trigger additional debris flows (Burtin et al., 2013).

2.1 Existing Warning System at the Illgraben

A series of 30 check dams (henceforth, individual check dams are referred to by the letters "CD" followed by a unique number, which increases in flow direction) has been installed along the lower 3.4 km of the Illgraben channel to stabilize the
15 channel along the current flow path and to minimize channel-bed and lateral erosion (Figures 1 and 2). Instrumentation consists of two separate systems, an observation station for data collection and an independent early warning system for the community. The observation station (Rickenmann et al., 2001, Hürlimann et al., 2003, McArdell et al., 2007) consists of geophones installed on check dams to detect time of passage, flow stage sensors (radar, laser, ultrasonic) to estimate the height of the flow, video cameras, an instrumented wall near the mouth of the channel (Berger et al., 2011), and a large force
20 plate situated under the roadway bridge near the mouth of the channel. This station is triggered by debris-flow passage (geophone) at a check dam located approx. 1 km upstream of the force plate and instrumented wall. The 8 m^2 force plate (McArdell et al., 2007) is currently configured to measure vertical and shear forces at a rate of 2 kH (McArdell, in press). Except for the force plate and instrumented wall, all instruments at the observation station are powered by batteries and solar panels.

The existing early warning system at the Illgraben was designed based on experience from the observation station. However, to ensure reliability it has subsequently been optimized to provide reliable early warning for the community (Badoux et al., 2009). The early warning system consists of three rain gauges within and surrounding the catchment, a geophone at the uppermost position in the catchment where instruments are expected to withstand rockfall activity, CD1 (Figure 1), and two
30 geophones and two radar stage sensors at CD9 and 10. Batteries and solar panels power the detection instruments. Warning consists of acoustic alarms and flashing lights installed at channel crossings frequented by tourists, and text messages delivered to the authorities.

The existing early warning system is contingent upon initial detection on the geophones at CD1, 9 and 10. Ideally, this is the geophone installed on CD1. Unfortunately, this system is prone to power outages due to limited sunlight and a weak GSM network signal. In contrast, detections at CD9 and 10 are deemed reliable and are less susceptible to potential damage by rockfall. CD10 also has a laser stage sensor and issues a warning when a predefined flow height is reached. For this warning,

5   delay time defined as the difference between initial detection and debris flow arrival at CD27, ranges from 0 to half an hour and is thus highly variable (Badoux et al., 2009). Finally, flow velocities estimated from propagation between CD10 and 29 typically lie between 1 and 8 m/s.

2.2 19 July 2011 Event

10   For the following analysis we investigate the seismic records of a debris flow event on 19 July 2011. On the lower debris fan, the event had a flow height of around 2 m and a flow velocity of about 2.3 m/s. With a total volume of around 30,000 m^3 it is classified as a small event. Initial geophone detection at CD1 occurred on 17:40:08, subsequent detection times are listed in Table 2. After the front passage, the event is characterized by pulse-like flow with around two dozens of "roll waves" arriving over the course of the 15-minute-long event (Figure 3). The individual waves are up to 1 m high, but their height is

15   variable and diminishes towards the end of the debris flow. The high percentage of fine material encountered in Illgraben debris flows is believed to be responsible for these roll waves (Rickenmann, 2001).

3 Seismic Data

During summer 2011, a temporary seismometer network (Fig. 1) was operational for about one hundred days (Burtin et al., 2013). Out of the recorded data, we analyze about 19 hours in the present study, including a debris flow event on 19 July

20   2011. The seismometers (labeled IGB1-IGB7, IGB9-IGB10; IGB8 was not fully functional on 19 July 2011) were powered by battery and solar energy (sensor and recording specifications are given in Table 1). Ground motion was sampled at 125 or 200 Hz and stored locally. The analysis presented here relies primarily on signal frequencies within the sensors' flat spectral response and for this reason digital counts are converted to ground motion with a single multiplication factor. More details on the seismic instrumentation were given by Burtin et al. (2013).

At IGB01, located near a catchment region where debris flows are believed to initiate (McArdell et al., 2007; Berger et al., 2011), the debris flow signal emerged above the seismic noise at around 17:35 (Figure 4A). Although the debris flow was rather small, it left a strong seismic footprint on all seismometers and occupies a broad seismic frequency range from below 1 to nearly 100 Hz (Figure 4C). The debris flow seismogram diminishes after around 30 minutes. After an additional 10-15

30   minutes, IGB01 recorded a second event. However, since this event cannot be identified on the other stations, it is likely a

local process, such as a landslide near IGB01 or a secondary debris flow, which did not propagate far enough downstream to be recorded at other stations.

Over the course of its duration, the debris flow signal undergoes amplitude variations for two reasons: first, a varying degree
5   of seismic energy generation related to flow velocity, channel topography and granulometry of entrained material and, second, the changing distance between moving material and recording seismometer. In theory, inter-particle collisions, particle hopping across the channel bed and turbulence in the water-sediment mixture emit seismic waves at all positions along the debris flow (Tsai et al., 2012; Gimbert et al., 2014). However, the primary seismic source is associated with the debris flow front (Burtin et al., 2014), where large boulders are mobilized (McArdell et al., 2007). This is in agreement with
10   independent studies of bedload transport suggesting that such large grain sizes dominate the energy transmission to the ground, even though their contribution to the overall mobilized volume is small (Turowski et al., 2015). The seismic signal strength can thus be used to trace the debris flow propagation through the seismometer network.

The debris flow has typical "cigar-shaped" signals, with seismogram envelopes emerging and fading out slowly (Figures 4
15   and 5). This gives an extended "tremor-like" appearance, in contrast to impulsive signals associated with e.g. earthquakes or explosions. Individual signal spikes likely represent impacts of large individual rocks or lateral landslides induced by the debris flow event (Burtin et al., 2013). The emergent character is also highlighted in Figure 5, which compares a 2-minute pre-event time series (Panel B) with part of the debris flow signal of the same length (Panel C). During such short time windows, neither amplitude modulation nor arrivals of individual seismic phases are visible making it difficult to distinguish
20   a debris flow record from seismic background noise. However, the relative amplitudes between stations show clear differences: In the pre-event noise record (Panel A), the Rhone Valley stations (IGB3, IGB9 and IGB10) have the largest amplitudes, most likely a consequence of anthropogenic noise. In contrast, during the debris flow record (Panel B), ground vibrations are largest in the Illgraben catchment, at Stations IGB01, IGB02 and IGB03. These temporal and spatial amplitude variations form the base of the detection and location scheme, which we now describe.

4 Detection and Location Scheme

Our proposed detection scheme for debris flow events uses continuous seismograms recorded with a seismometer network installed throughout the catchment and fan of a given debris-flow prone torrent. The approach aims to satisfy the following demands:
30

1. Detection and location of debris flow initiation and front position have to be rapid and reliable.

2. No individual seismic phase arrivals are available for locating the source.

3. No seismic velocity model is available for the torrent catchment.

4. Throughout the network, debris flow seismograms are poorly correlated.

Point 1 is generally desirable for early warning systems, which should avoid false alarms triggered by seismic noise sources

5   outside the torrent. Point 2 results from the general emergent, tremor-like or cigar-shaped appearance of debris flow
seismograms and other mass motion events such as landslides and avalanches (Burtin et al., 2013). In Point 3, it is
recognized that the shallow subsurface structure of Alpine terrain is highly heterogeneous and difficult to model. Together,
Points 2 and 3 imply that arrival time inversion of discernable seismic phases, typically used for locating earthquakes (e.g.
Diehl et al., 2009) is not possible for debris flow seismograms. In principle, array-based location schemes can compensate

10   for the lack of seismic phase arrivals by exploiting signal coherence (e.g. Rost and Thomas, 2002). However, in debris flow
applications, local topography and heterogeneous near-surface structure lead to a loss in signal coherence throughout the
seismic network (Point 4). Our attempt to use signal coherence for locating the seismic source associated with the debris
flow front were consequently unsuccessful.

15   In order to meet the requirements of Points 1-4, we follow the method of Battaglia and Aki (2003) to locate the source of
tremor-like seismic signals via differences in amplitudes throughout the recording array. This approach was originally
developed for volcano seismology. It has recently been adapted to locate fracture events and hydraulic tremor on ice sheets
(Jones et al., 2013; Röösli et al., 2014), and the same principle was used by Burtin et al. (2016) to analyze different degrees
of seismic energy excitation during debris flow events.

In the far field, the amplitude A_i of a seismic signal recorded at the ith station follows the decay relationship

$$A_i(r) = \frac{A_0}{r_i^{\,n}} e^{-\alpha r_i} \qquad\qquad (1)$$

25   where r is the source-station distance, A_0 is the signal amplitude at the source (henceforth "source strength"), α is the signal
decay constant and n=1 for body waves and n=1/2 for surface waves (Battaglia and Aki, 2003). Equation (1) describes
amplitude decay in the far field, whereas a rigorous representation of source strength naturally has to take into account the
near field. Consequently, A_0 may be interpreted as parameterized source strength but lacks a strict physical meaning. In fact,
directly at the source location (at r=0), A_i becomes infinite and A_0 is undefined.

30

In Equation 1, the exponential term accounts for anelastic damping of the seismic wave, whereas the $1/r^n$ factor describes
amplitude attenuation due to geometric spreading. The decay constant α can be expressed as

$$\alpha = \frac{\pi f}{Q\beta} \qquad (2)$$

where f is the signal frequency, Q is the seismic quality factor and β the seismic wave velocity.

5   We calculate the signal's root mean square (RMS) amplitudes at each recording station for a specified time window. The RMS is a time-averaged strength measure of the debris flow signal and its spatial variations throughout the array are therefore subject to Equation 2. Consequently, by matching measured spatial RMS distribution with the predictions of Equation 1, we can identify the source location of the debris flow signal. It should be stressed that in volcanic applications, site amplification (or damping) demand seismic signal correction prior to application of Equation 1 (Aki and Ferrazzini, 10   2000; Battaglia and Aki, 2003). However, as shown below, we found that with the available Illgraben data our debris flow source could be located without signal correction and we therefore refrained from analysis of site effect.

We assume the case of body waves (Burtin et al., 2013) and approximate the path traveled by seismic waves between debris flow front and seismometer by straight lines. For our decay-fit locations, the geographic location and source strength of the 15   debris flow front is varied in a grid search. Moreover, we vary the decay constant α in the range expected for body wave velocities and Q values near the Earth's surface (Burtin et al., 2013). Ground motion amplitude is estimated via the root-mean-square of 100-second seismogram time windows and the fit quality is quantified with the variance reduction defined as

$$VR = \left(1 - \frac{\sum(data - fit)^2}{\sum(data^2)}\right) * 100\% \qquad (3)$$

In a spatial grid search over geographic coordinates, the maximum in variance reduction (100% represents a perfect fit) indicates the source of the recorded seismic signal. The absolute upper limit (100%) facilitates interpretation of fit quality and its variation at different times. The disadvantage of using variance reduction as an indicator for fit quality is that for a monotonic fitting function such as Equation (1), even poor fits may provide relatively high variance reductions (~80% as 25   shown below).

5 Results: Seismic Noise Sources and Debris Flow Locations

Prior to decay fit location, we apply a two-pole 0.5-5 Hz Butterworth bandpass filter to the seismic time series, acknowledging that the debris flow seismograms primarily exhibit higher frequencies (Figure 4). However, this frequency range is a compromise between minimizing effects of spatial differences in decay constant α and staying near a range where 30   the debris flow transmits seismic energy and the frequency response of our sensors is flat (Table 1).

The results of fitting decay curves (Equation 1) to consecutive 100 s amplitude averages on 19 July 2011 (including the debris flow event) are illustrated in the animated movie in the supplemental material (http://people.ee.ethz.ch/~fwalter/download/movies/movie_df.mov), in Figure 6 and in Figure 7. Between 01:00 and 04:00,

5 the variance reduction lies between 80 % and 90 % and calculated seismic source strength is low. Consequently, even in the absence of a dominant seismic source, variance reductions above 80 % can be expected. At around 04:00, the variance reduction rises and reaches up to 100% and the source strength increases as well, though by less than an order of magnitude. This marks the influence of a noise source, whose signal is detectable on station IGB07 in the upper Illgraben catchment as well as station IGB09 on the debris fan (Figures 6C and 7C). Decay-curve fitting locates the source of this persistent noise

10 signal between IGB03 and IGB10 within or near the village of Susten, suggesting an anthropogenic noise source. Despite temporary drops in variance reduction to 80% or lower accompanied by drops in source strength (Figure 8), this source continues dominating the noise field throughout the afternoon.

After 15:00, the noise source strength fades and fluctuating variance reductions indicate that there no longer exists a single

15 noise source dominating the entire array. Near 17:35, the variance reduction and the source strength increase, the latter drastically by almost two orders of magnitudes. This marks the beginning of the debris flow event. The signal source locates high up in the catchment area of the Illgraben torrent (Figure 6 and movie in the supplemental material). During most of the following 100-second time windows, the decay fit determines locations with variance reductions near 100%.

20 During the debris flow event, the decay-fit locations move downstream at an average of 1.8 m/s (movie in the supplemental material and Figure 9). For comparison, the geophone-derived arrival times at CD1, 10, 24 and 27 yield an average velocity of 2.9 m/s (Fig. 9). Furthermore, whereas the CD1 arrival time for the geophone detection and the seismic decay-fit location nearly coincide, the arrival time differences grow as the debris flow moves downstream. At CD24 the decay-fit arrival time lacks 10 minutes behind geophone detection. We interpret this discrepancy to result from changes in seismogenic processes

25 within the debris flow: near the initiation, the debris flow front primarily transmits the seismic energy. Subsequently, later arriving parts participate in the seismic transmission biasing the decay fit locations backward from the debris flow front. This interpretation is supported by later arriving roll waves (Figure 3), each transmitting seismic energy, as well as typical changes in longitudinal debris flow profiles, which become progressively less steep and thus stretched out during propagation (Berger et al., 2011).

30

The distance from the variance reduction maximum to the Illgraben channel varies between below 100 m and nearly 900 m (Figure 9B). Assuming that the debris flow source is confined to the channel, these numbers provide an approximate measure for location uncertainty. During the debris flow, the decay constant α takes values within the entire grid search range (0 - 0.001 m^{-1}). In view of the local topography and ground structure heterogeneities within the grid search area, it is

difficult to interpret the spatially averaged value for α and its variations. However, they likely do carry physical meaning, because when fixing α=0, variance reductions drop by 10-20% during several 100 s time windows.

During the first 5 minutes of the debris flow, the seismic source strength grows slowly (Figure 9A). Between 17:31 and
5   17:32, the source strength reaches 1.8×10^{-4} m/s and thus exceeds the strength of other seismic sources in the upper catchment measured earlier in the 19-hour record (Figure 8B). By 17:40:01, near the time of geophone detection at CD1 (17:40:08; Table 2), seismic source strength of the debris flow has increased by around an order of magnitude.

We conclude that at 17:32, the decay fit unmistakably locates the debris flow source to the Illgraben catchment with stronger
10   source amplitude than during previous 100 s time windows. About 8 minutes later, the decay fit locates the debris flow source at CD1, which is confirmed by the independent geophone detection. Consequently, we interpret 17:32 as the earliest seismic detection time of the debris flow with our decay-fit approach.

6 Discussion: Detectability and Background Noise

Since the present detection scheme relies entirely on amplitude information and neglects signal phase, its success is
15   particularly dependent on levels of seismic background noise. Only stations where the debris flow signal emerges above the background noise level are of use to the decay fit.

We evaluate how changes in seismic background noise may affect debris flow detectability by comparing seismic signal strengths recorded at IGB09 and IGB10 to a noise record of the additional seismometer station IGN01 (Figure 1). This
20   station (Type Lennartz LE 3D 5s sensor; flat frequency response: 0.2-50 Hz; sampling frequency: 200 Hz) was operational between 27 May 2015 and 16 July 2015 and was installed in the Rhone Valley, some 500 m west of the Illgraben channel. The original purpose of this station was to record a debris flow seismogram in a quieter location than stations IGB09 and IGB10, which, according to our decay fit locations, were installed closer to dominant anthropogenic noise sources. Unfortunately, no debris flow occurred during the deployment of station IGN01. Nevertheless, this station's record is well
25   suited for a comparison with background noise at the other Rhone Valley stations IGB09 and IGB10.

To characterize the background noise floor and its variations, we followed the procedure of McNamara and Buland (2004). We divided the continuous record of IGB09, IGB10 and IGN01 into 10-minute long windows and for each window we calculate the power spectral density (PSD) from the Discrete Fourier Transform. PSD was calculated in units of decibel with
30   a reference ground velocity of 1 m/s. The hourly averages of the 10-minute PSD's are subsequently distributed between -100 and 200 dB into 0.5 dB-wide bins from which probability density functions (PDF's) of PSD are calculated.

Figure 10A shows the 51-day-long noise PSD-PDF recorded at IGN01 and the mean and standard deviation of the 19-hour-long noise PSD-PDF recorded at IGB10, which includes the debris flow. At both stations, the noise level is comparable, while peak probabilities in the IGN01 PSD-PDF lie below one standard deviation of the IGB10 noise mean. This supports the expectation that during substantial time periods, IGN01 is quieter than IGB10. Figure 10B shows again the 51-day-long

5   noise PSD-PDF of IGN01 together with the debris flow spectra recorded at stations IGB09 and IGB10. Within the 1-5 Hz frequency range relevant for our decay fit locations, the PSD-PDFs show two branches in noise amplitude (marked with two arrows). The branches are separated by up to 12 dB and reconnect above 5 Hz. Extracting PSD curves, which are bundled in the upper PDF branch (not shown) associates this stronger branch with typical working hours during the week and thus the main contribution of anthropogenic noise. However, the 19 June 2011 debris flow signal recorded at IGB09 and IGB10

10   dominates this anthropogenic noise more than 90% of the 51-day deployment period of IGN01 (Figure 10C).

This noise analysis uses a single spectral representation of the debris flow seismogram averaged over the entire event duration. Nonetheless, it does indicate that the 19 June 2011 debris flow dominates the seismic spectrum compared to continuous records of seismic background noise. We conclude that for debris flow events, whose seismic source strengths are at least as high as the 19 June 2011 event, and which are recorded at some distance from roads or settlements (e.g. at the

15   site of IGN01), anthropogenic noise does not affect detectability with the decay fit scheme proposed here.

In this detectability analysis we assumed that background noise did not change significantly between deployment periods of stations IGB09 and IGB10 (2011) and station IGN01 (2015). New or temporary construction sites, differences in traffic flow

20   or other factors would violate this assumption and argue once more for valley seismometer installations away from the village of Susten or the main highway parallel to the Rhone River (Figure 1). Ideally, a noise analysis should be constantly updated and repeated throughout a monitoring period.

6.1 Suitability for Early Warning

The proposed detection and location scheme for debris flows relies on a seismic network installed throughout a torrent's

25   catchment. Applied to a relatively small debris flow event from the Illgraben, Switzerland, our method is capable of quickly detecting and locating debris flow initiation and to trace its propagation downstream. Event initiation is marked by a sudden increase in seismic source strength and a successful fit of ground vibration decay indicated by nearly 100 % variance reductions of decay fit. Compared to the currently first detection point at CD1, event recognition could thus be improved by an amount equal to the propagation time between debris flow initiation and arrival at CD1. For the present example, this

30   improvement is around 8 minutes. However, in practice the improvement is larger, because current instrumentation in and near the upper channel (including CD1) does not operate reliably as a result of local limitation in GSM network access and solar power. In general, seismometer installations such as presented here can be placed away from the channel in sites with

enough sunlight or better GSM network reception. This offers more flexibility of instrumentation compared to existing in-channel installations.

The advantage of our approach is that instead of relying on arrival times of specific seismic phases or on signal coherence, it uses time-averaged ground vibration amplitudes. Thus, detection and location are achieved in a single step via a simple grid search algorithm without the need for a seismic velocity model. Our grid search is currently implemented in Matlab® and runs on a single processor. It takes less than 3 s to process a 100 s time window. This time could be further reduced by distributing computation on several processors and/or by limiting the grid search to the vicinity of the torrent channel. Similarly, a search domain, which avoids locations, where seismometers reside in the near field would reduce the grid space in addition to providing numerical stability.

Apart from amplitude averaging and bandpass filtering, no time-consuming preprocessing steps are necessary for our decay-fit location. The amplitude averages furthermore decrease the data volume by several orders of magnitudes considering that raw seismic data are often sampled at hundreds of Hz. Requirements for data transfer between seismic stations and a central computer are thus significantly reduced. Somewhat surprisingly, no seismic signal correction for amplification at individual seismometer sites was necessary to achieve our locations of the debris flow front. In future studies, signals from tectonic earthquakes or artificial explosions could be used to correct for such site effects and thus improve location accuracy (Aki and Ferrazzini, 2000; Battaglia and Aki, 2003).

Our detector aims to be instantaneous in the sense that no additional time series prior to or after the time window used for amplitude averaging is necessary. In theory, this eliminates the need for a pre-event noise window such as required for the STA/LTA algorithm (Sleeman et al., 1999). However, it has yet to be investigated if the variance reduction and source strength thresholds derived from the data displayed in Figure 8 are generally valid. This can only be tested with additional data from debris flows of various sizes.

The proposed decay fit combines amplitude information from all stations directly in the detection and location scheme. Single-trace detectors demand an additional step, which associates detections from several stations to an event and require site-specific tuning and longer time series for reliable performance. More sophisticated detection methods based on stochastic seismic event recognition have the advantage to automatically tune themselves based on only a limited training data set (Hammer et al., 2012). However, these algorithms also require a large portion of the debris flow seismogram in order to accurately describe the characteristic signal states and transitions between them. Furthermore, the computational expenditure for these algorithms is non-negligible.

In summary, the above advantages could be leveraged in real-time debris flow detection with continuous seismic data streams. Performance of our proposed event detection and location method is encouraging, yet implementation of a reliable early warning system has to tackle additional practical challenges. Perhaps most importantly, our approach still depends on reliable data communication via the GSM network. Although seismometers offer more flexible installations, the topography

5   of the Illgraben catchment does affect GSM network reception. This likely imposes some constraints on our method, which are best investigated with future test deployments.

7 Conclusion

The presented seismic detection scheme for debris flow events focuses exclusively on averaged amplitude information. This allows for efficient seismic source location and consequently rapid detection of debris flow initiation as soon as it dominates

10 the ground vibration throughout our seismic network. Technical challenges for data communication and processing remain and our approach would clearly benefit from concurrent monitoring with independent methods. Notwithstanding, the decay fit technique successfully detected the initiation of the 19 June 2011 debris flow event and traced the propagation of its front towards the valley. The simple and efficient decay-fit processing reduces user interaction and requires no seismic velocity model or instrumentation in hazardous terrain next to the torrent. Consequently, this makes our approach a promising

15 candidate for early warning systems against debris flow hazards.

Acknowledgements

The salary of FW was partially covered by the SNF grant PP00P2_157551. The SEIS-UK equipment pool (NERC) and the École et Observatoire des Sciences de la Terre de Strasbourg provided the seismic stations deployed during summer 2011. We thank Jérôme Vergne for help with instrumentation and network planning. Seismic equipment and data archiving

20 facilities for station IGN01 were provided by the Swiss Seismological Service.

References

Aki, K., & Ferrazzini, V. (2000). Seismic monitoring and modeling of an active volcano for prediction. *Journal of Geophysical Research: Solid Earth*, *105*(B7), 16617-16640.

Arattano, M., & Marchi, L. (2005). Measurements of debris flow velocity through cross-correlation of instrumentation data. *Natural Hazards and Earth System Science*, *5*(1), 137–142. http://doi.org/10.5194/nhess-5-137-2005

Arattano, M., Abancó, C., Coviello, V., & Hürlimann, M. (2014). Processing the ground vibration signal produced by debris flows: The methods of amplitude and impulses compared. *Computers and Geosciences*, *73*, 17–27. http://doi.org/10.1016/j.cageo.2014.08.005

5   Battaglia, J., & Aki, K. (2003). Location of seismic events and eruptive fissures on the Piton   de la Fournaise volcano using seismic amplitudes. *Journal of Geophysical Research: Solid Earth*, *108*(B8).

Berger, C., McArdell, B. W., & Schlunegger, F. (2011). Direct measurement of channel erosion by debris flows, Illgraben, Switzerland. *Journal of Geophysical Research: Earth Surface*, *116*(1), 1–18. http://doi.org/10.1029/2010JF001722/

Burtin, A., Bollinger, L., Vergne, J., Cattin, R., & Nábělek, J. L. (2008). Spectral analysis of seismic noise induced by rivers: A new tool to monitor spatiotemporal changes in stream hydrodynamics. *Journal of Geophysical Research: Solid Earth*, *113*(B5).

15   Burtin, A., Hovius, N., McArdell, B. W., Turowski, J. M., & Vergne, J. (2014). Seismic constraints on dynamic links between geomorphic processes and routing of sediment in a steep mountain catchment. *Earth Surface Dynamics*, *2*(1), 21–33. http://doi.org/10.5194/esurf-2-21-2014.

Burtin, A., Hovius, N., & Turowski, J. M. (2016). Seismic monitoring of torrential and fluvial processes. *Earth Surface Dynamics*, *4*(2), 285–307. http://doi.org/10.5194/esurf-4-285-2016.

Dammeier, F., Moore, J. R., Haslinger, F., & Loew, S. (2011). Characterization of alpine rockslides using statistical analysis of seismic signals. *Journal of Geophysical   Research: Earth Surface*, *116*(F4).

25   Deganutti AM, Marchi L, Arattano M (2000) Rainfall and debris-flow occurrence in the Moscardo basin (Italian Alps). In: Wieczorek GF, Naeser ND (eds) Debris-flow hazards mitigation: mechanics, prediction, and assessment. A.A. Balkema, Rotterdam, pp 67–72.

Deparis, J., Jongmans, D., Cotton, F., Baillet, L., Thouvenot, F., & Hantz, D. (2008). Analysis of rock-fall and rock-fall
30   avalanche seismograms in the French Alps. *Bulletin of the Seismological Society of America*, *98*(4), 1781-1796.

Fan J-C, Liu C-H, Wu M-F, Yu SK (2003) Determination of critical rainfall thresholds for debris-flow occurrence in central Taiwan and their revision after the 1999 Chi-Chi great earthquake. In: Rickenmann D, Chen CL (eds) Debris-flow hazards mitigation: mechanics, prediction, and assessment. Millpress, Rotterdam, pp 103–114.

Gimbert, F., Tsai, V. C., & Lamb, M. P. (2014). A physical model for seismic noise generation by turbulent flow in rivers. *Journal of Geophysical Research: Earth Surface*, *119*(10), 2209-2238.

Hammer, C., Beyreuther, M., & Ohrnberger, M. (2012). A Seismic-Event Spotting System for Volcano Fast-Response Systems. *Bulletin of the Seismological Society of America*, *102*(3), 948-960.

Hübl, J., Kogelnig, A., Suriñach, E., Vilajosana, I., & Mcardell, B. W. (2012). A review on acoustic monitoring of debris flow. *WIT Transactions on Engineering Sciences*, *73*(2), 73–82. http://doi.org/10.2495/DEB120071.

Hürlimann, M., Rickenmann, D., & Graf, C. (2003). Field and monitoring data of debris-flow events in the Swiss Alps. *Canadian Geotechnical Journal*, *40*(1), 161–175. http://doi.org/10.1139/t02-087.

Jones, G. A., Kulessa, B., Doyle, S. H., Dow, C. F., & Hubbard, A. (2013). An automated approach to the location of icequakes using seismic waveform amplitudes. *Annals of Glaciology*, *54*(64), 1-9.

Manconi, A., M. Picozzi, V. Coviello, F. De Santis, and L. Elia (2016), Real-time detection, location, and characterization of rockslides using broadband regional seismic networks, Geophysical Research Letters, 43, doi:10.1002/2016GL069572.

McArdell, B. W., Bartelt, P., & Kowalski, J. (2007). Field observations of basal forces and fluid pore pressure in a debris flow. *Geophysical Research Letters*, *34*(7), 2–5. http://doi.org/10.1029/2006GL029183.

McArdell, B.W. (in press). Field Measurements of Forces in Debris Flows at the Illgraben: Implications for Channel-Bed Erosion. *International Journal of Erosion Control Engineering*.

McNamara, D. E., & Buland, R. P. (2004). Ambient noise levels in the continental United States. *Bulletin of the seismological society of America*, *94*(4), 1517-1527.

Pierson TC (1986) Flow behaviour of channelized debris flows, Mount St. Helens, Washington. In: Abra- hams AD (ed) Hillslope processes. Allen & Unwin, Boston, pp 269–296.

Rickenmann, D., & Zimmermann, M. (1993). The 1987 debris flows in Switzerland: documentation and analysis. *Geomorphology*, *8*(2-3), 175–189. http://doi.org/10.1016/0169-555X(93)90036-2.

Rickenmann, D., Hürlimann, M., Graf, C., Näf, D., & Weber, D. (2001). Murgang-Beobachtungsstationen in der Schweiz. *Wasser, Energie, Luft*. In German. Retrieved from http://www.slf.ch/wsl/info/mitarbeitende/grafc/pdf/4110.pdf.

Röösli, C., Walter, F., Husen, S., Andrews, L. C., Lüthi, M. P., Catania, G. A., & Kissling, E. (2014). Sustained seismic tremors and icequakes detected in the ablation zone of the Greenland ice sheet. *Journal of Glaciology*, *60*(221), 563-575.

Rost, S., & Thomas, C. (2002). Array seismology: Methods and applications. *Reviews of geophysics*, *40*(3).

Schimmel, A., & Hübl, J. (2015). Automatic detection of debris flows and debris floods based on a combination of infrasound and seismic signals. *Landslides*, (April). http://doi.org/10.1007/s10346-015-0640-z.

Sleeman, R., & van Eck, T. (1999). Robust automatic P-phase picking: an on-line implementation in the analysis of broadband seismogram recordings. *Physics of the earth and planetary interiors*, *113*(1), 265-275.

Suriñach, E., Sabot, F., Furdada, G., & Vilaplana, J. (2000). Study of seismic signals of artificially released snow avalanches for monitoring purposes. *Physics and Chemistry of the Earth, Part B*, *25*(9), 721–727. http://doi.org/10.1016/S1464-1909(00)00092-7.

Tsai, V. C., Minchew, B., Lamb, M. P., & Ampuero, J. P. (2012). A physical model for seismic noise generation from sediment transport in rivers. *Geophysical Research Letters*, *39*(2).

Turowski, J. M., Wyss, C. R. and Beer, A. R. (2015). Grain size effects on energy delivery to the streambed and links to bedrock erosion. *Geophysical Research Letters*, 42, 1775-1780.

Wieczorek GF (1987) Effect of rainfall intensity and duration on debris flows in central Santa Cruz Mountains, California. In: Costa JE, Wieczorek GF (eds) Debris flows/ avalanches: process, recog- nition and mitigation. *Reviews in engineering geology*, vol 7. Geological Society of America, Boulder (CO), pp 93–104.

TABLES

Station name	Sensor type	Range of flat frequency response (Hz)	Sampling frequency (Hz)
IGB01	Güralp CMG-6TD	1-100	200
IGB02	Güralp CMG-40T	0.033-50	125
IGB03	Güralp CMG-6TD	1-100	200
IGB04	Güralp CMG-6TD	1-100	200
IGB05	Güralp CMG-6TD	1-100	200
IGB06	Güralp CMG-6TD	1-100	200
IGB07	Güralp CMG-6TD	1-100	200
IGB09	LE-3Dlite	1-100	200
IGB10	LE-3Dlite	1-100	200

Table 1: Specifications for seismic network instrumentation used in detection and location scheme of the present analysis.

Check Dam ID	Arrival Time
CD1	17:40:08
CD10	17:43:10
CD24	17:55:48
CD27	17:58:22
CD29	18:02:16

Table 2: Arrival times of debris flow front at check dams instrumented with geophones.
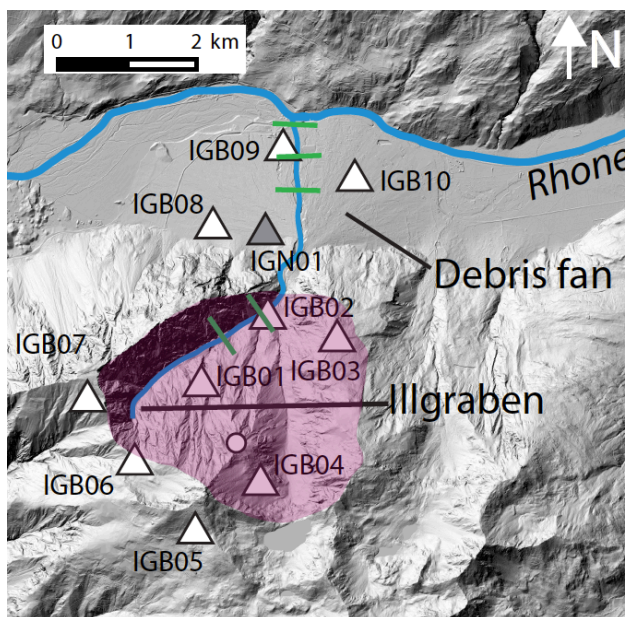
Figure 1: Illgraben region with its upper catchment area (shaded polygon) and debris fan in the Rhone Valley. Green lines represent Check Dams 1, 10, 24, 27 and 27, seismometer locations are indicated by triangles (grey triangle represents the 2015 noise record station) and a WSL rain gauge is indicated by the circle.

Figure 2: Photo of Illgraben debris flow event near Check Dam 28. Source: Brian McArdell, WSL.
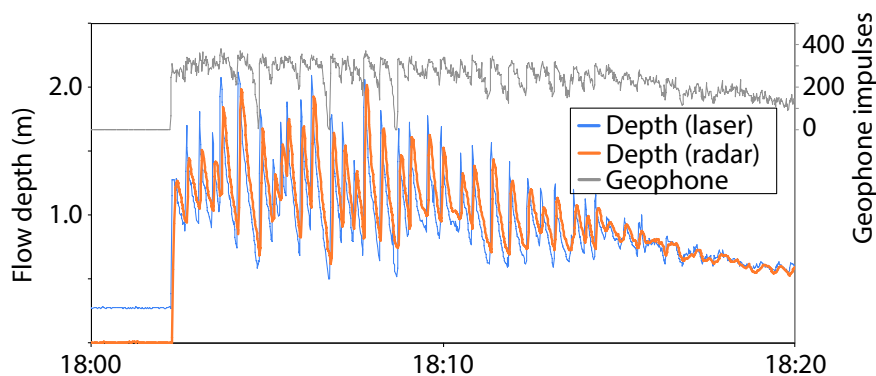
Figure 3: Flow depth and geophone impulses of Illgraben debris flow event on 19 July 2011 (recorded near Check Dam 29).
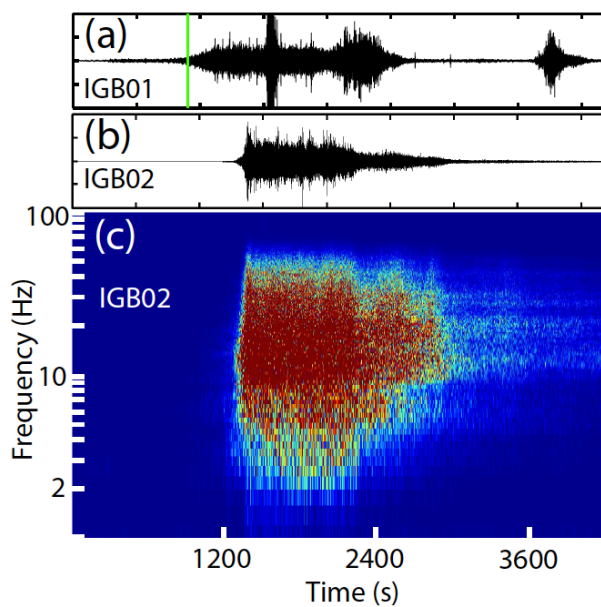
Figure 4: Debris flow seismograms at stations IGB01 and IGB02 (Panels a and b, respectively) and spectrogram of station IGB02 (c). Green bar in Panel a denotes 17:35 on 19 July 2011. Note the second seismic burst after 3600 s likely representing a local mass motion event near IGB01.
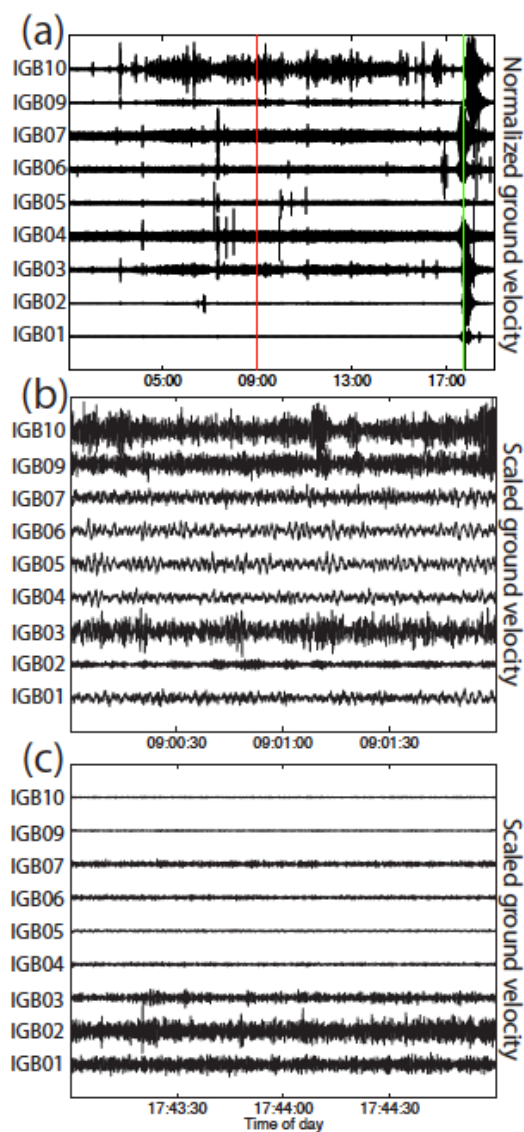
Figure 5: Debris flow seismograms and pre-event noise for the event on 19 June 2011. (a) Record showing the debris flow event around 18:00 and pre-event background noise. (b) and (c) show two-minute long records at the time instances denoted by the red and green bars in Panel (a).
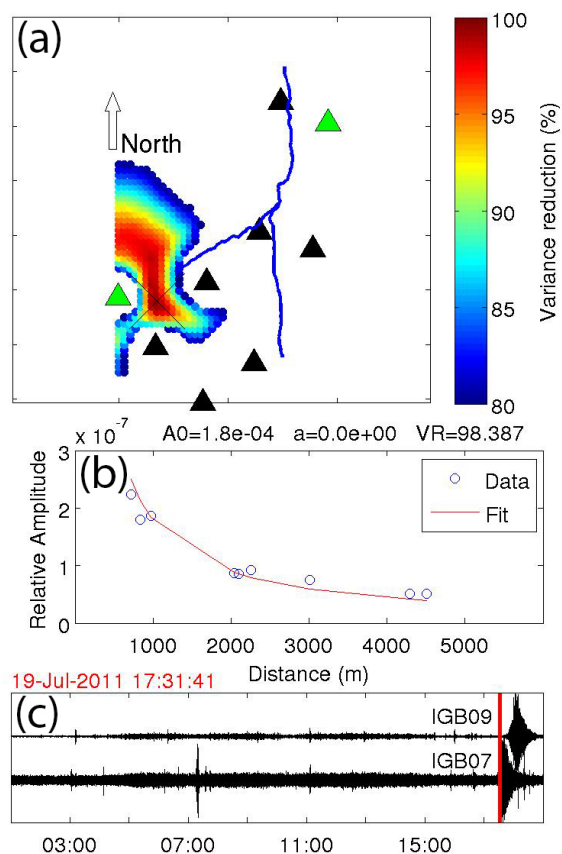
Figure 6: Decay-fit location of debris flow front at the initiation of the event. (a) shows the seismic network, the torrent bed (blue line) and color-coded grid locations for variance reductions exceeding 80%. Black cross indicates best-fit location. (b) shows the amplitude attenuation fit associated with the best-fit location. (c) shows the time instance (red bar) on an Illgraben catchment seismometer record (IGB07) and a Rhone Valley seismometer record (IGB09), both marked in Panel A with green triangles (IGB07: southern station, IGB09: northern station).
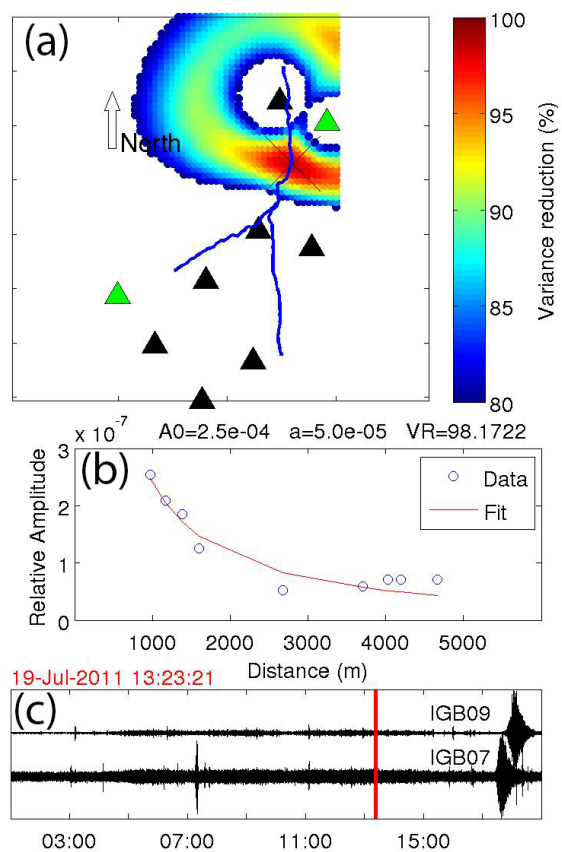
Figure 7: Same as Figure 6, except during a noise window before the debris flow event.
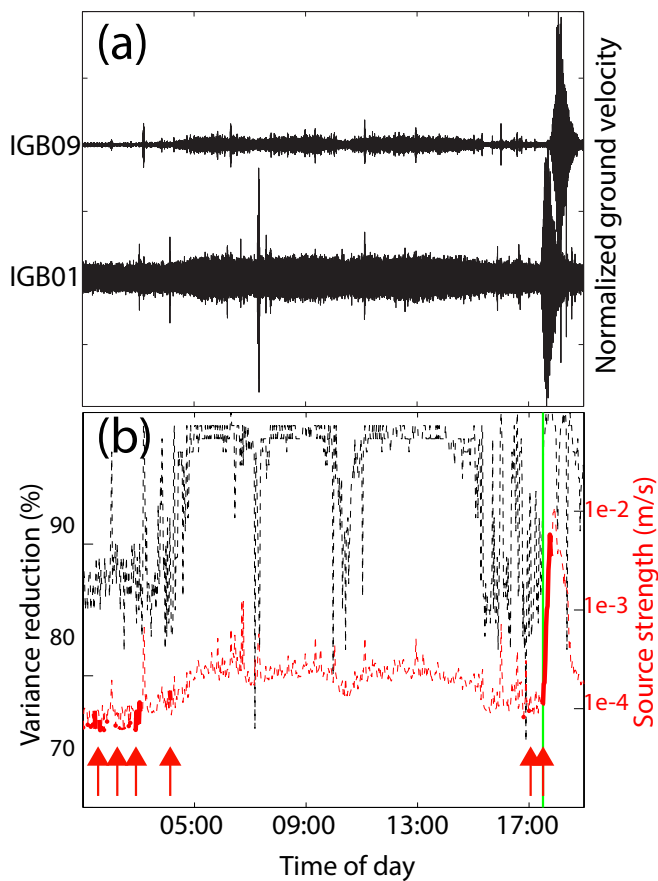
Figure 8: Results of the amplitude decay-fit location. (a) Seismograms of stations IGB01 (in the Illgraben catchment) and IGB09 (in the Rhone Valley). (b) Variance reduction (black) and equivalent source strength (red). Thick solid red lines denote time instances when the best fit location lies in the Illgraben catchment (also indicated with red arrows), dashed lines denote the remaining time instances. The green line marks 17:30 near the debris flow initiation time.
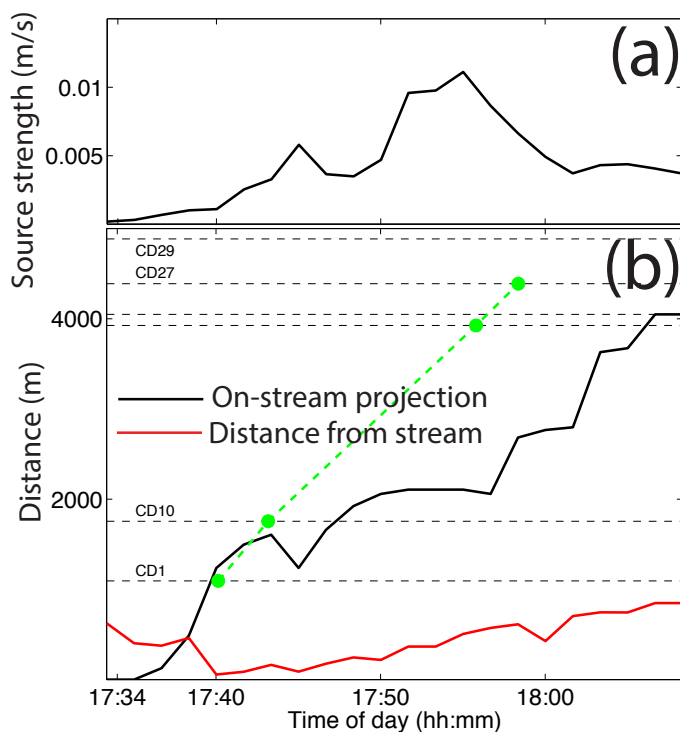
Figure 9: Best-fit source locations and source strength of the debris flow seismicity. (a) Temporal evolution of source strength. (b) Black line shows the location projected onto the along-flow coordinate of the stream. Red line shows the distance of the best-fit location from the streambed. Green dots connected by dashed lines indicate check dam arrival times (Check Dam 24 and 25 labels are omitted for clarity).
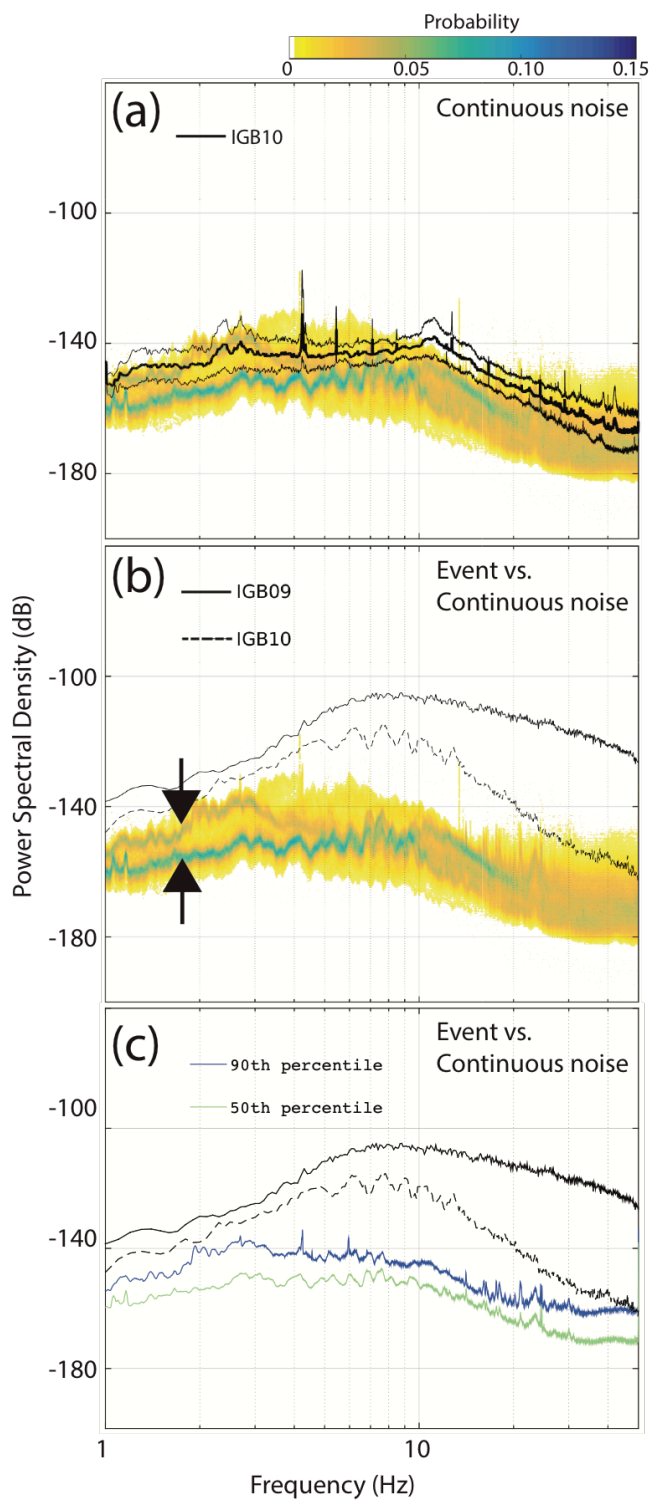
Figure 10: Debris flow spectra recorded at IGB09 and IGB10 together with probabilistic spectral representation of a 3-months noise time window recorded between 27 May and 16 July 2015 at station IGN01 ("PSD-PDF"). (a) Comparison between noise PSD-PDFs at IGN01 and noise mean and standard deviation at IGB10 (thick and thin black lines, respectively). (b) Noise PSD-PDF of station IGN01 and debris flow spectra of IGB09 and IGB10. Black arrows point to the two PDF branches discussed in the main text. (c) Debris flow spectra at IGB09 and IGB10 with 50th and 90th percentile of noise PSD-PDF of IGN01. Note that at both stations (IGB09 and IGB10), the debris flow signal dominates the seismic noise measured at IGN01 over the entire shown frequency range (1-14 Hz).